THE JOURNAL OF BIOLOGICAL CHEMISTRY VOL. 287, NO. 15, pp. 12050–12059, April 6, 2012

TRIM67 Protein Negatively Regulates Ras Activity through Degradation of 80K-H and Induces Neuritogenesis*[S]

Received for publication, September 26, 2011, and in revised form, February 13, 2012 Published, JBC Papers in Press, February 15, 2012, DOI 10.1074/jbc.M111.307678

Hiroaki Yaguchi[‡§], Fumihiko Okumura[‡], Hidehisa Takahashi[‡], Takahiro Kano[‡§], Hiroyuki Kameda[‡], Motokazu Uchigashima[¶], Shinya Tanaka[‖], Masahiko Watanabe[¶], Hidenao Sasaki[§], and Shigetsugu Hatakeyama[‡1]

From the Departments of [‡]Biochemistry, [§]Neurology, [¶]Anatomy, and [‖]Pathology, Hokkaido University Graduate School of Medicine, Sapporo, Hokkaido 060-8638, Japan

Background: TRIM67, which is selectively expressed in the cerebellum, is a novel member of the TRIM protein family.
Results: TRIM67 interacts with PRG-1 and 80K-H, which is involved in the Ras-mediated signaling pathway.
Conclusion: TRIM67 regulates Ras signaling via degradation of 80K-H, leading to neural differentiation including neuritogenesis.
Significance: Analysis of TRIM67 would provide therapeutic benefits for neurodegenerative diseases.

Tripartite motif (TRIM)-containing proteins, which are defined by the presence of a common domain structure composed of a RING finger, one or two B-box motifs and a coiled-coil motif, are involved in many biological processes including innate immunity, viral infection, carcinogenesis, and development. Here we show that TRIM67, which has a TRIM motif, an FN3 domain and a SPRY domain, is highly expressed in the cerebellum and that TRIM67 interacts with PRG-1 and 80K-H, which is involved in the Ras-mediated signaling pathway. Ectopic expression of TRIM67 results in degradation of endogenous 80K-H and attenuation of cell proliferation and enhances neuritogenesis in the neuroblastoma cell line N1E-115. Furthermore, morphological and biological changes caused by knockdown of 80K-H are similar to those observed by overexpression of TRIM67. These findings suggest that TRIM67 regulates Ras signaling via degradation of 80K-H, leading to neural differentiation including neuritogenesis.

The ubiquitin-mediated proteolytic pathway has an important role in the elimination of short-lived regulatory proteins (1), including those that contribute to the cell cycle, cellular signaling in response to environmental stress or extracellular ligands, morphogenesis, secretion, DNA repair, and organelle biogenesis (2). The system responsible for the attachment of ubiquitin to the target protein consists of several components that act in concert (3, 4), including a ubiquitin-activating enzyme (E1), a ubiquitin-conjugating enzyme (E2) and a ubiquitin-protein isopeptide ligase (E3). E3 is thought to be the component of the ubiquitin conjugation system that is most directly responsible for substrate recognition (4). On the basis of structural similarity, E3 enzymes have been classified into three families: the HECT (homologous to E6-AP C terminus)[2] family (2, 5), the RING finger-containing protein family (6–8), and the U-box family (9–11). The superfamily of tripartite motif-containing (TRIM) proteins is defined by the presence of a tripartite motif composed of a RING domain, one or two B-box motifs and a coiled-coil region (12, 13). Many TRIM proteins are induced by type I and type II interferons (IFNs), suggesting that TRIM proteins have an important role in antiviral and anti-microbial systems (14).

It has been reported that TRIM9 is highly expressed in the cerebral cortex in mouse and human brains and that TRIM9 is decreased in damaged brains in patients who have Parkinson disease and dementia with Lewy bodies (15). TRIM9 plays an important role in the regulation of neuronal functions and participates in the pathological process of Lewy body disease (15). Overexpression of the *Caenorhabditis elegans* homolog of TRIM9 induces ventral axon outgrowth and ectopic branching in anterior lateral microtubule (ALM) mechanosensory neurons (16). *C. elegans TRIM9* is important for axon ventral guidance in response to the attractive UNC-6/Neritin-1 signal, and *Drosophila* TRIM9 is required for Netrin-mediated midline attraction of sensory axons (17).

Protein kinase C substrate 80K-H (80K-H), also known as glucosidase II β, which encodes a soluble protein rich in glutamic and aspartic acid with putative endoplasmic reticulum (ER) retention signal at the C-terminal region (18), has been identified as a molecule downstream of fibroblast growth factor receptor (FGFR) 1 and keratinocyte growth factor receptor (19). 80K-H directly binds activated FGFR1 and forms a ternary complex with growth factor receptor-bound protein 2 (GRB2) and son of sevenless (SOS) (19). This complex formation is

* This work was supported in part by Grants-in-Aid for Scientific Research from the Ministry of Education, Culture, Sports, Science, and Technology.
[S] This article contains supplemental Fig. S1.
[1] To whom correspondence should be addressed: Department of Biochemistry, Hokkaido University Graduate School of Medicine, Kita15, Nishi7, Kita-ku, Sapporo 060-8638, Japan. Tel.: 81-11-706-5047; Fax: 81-11-706-5169; E-mail: hatas@med.hokudai.ac.jp.

[2] The abbreviations used are: HECT, homologous to E6-AP COOH terminus; ALM, anterior lateral microtubule; CaM, calmodulin; EPSC, excitatory postsynaptic current; ER, endoplasmic reticulum; FGFR, fibroblast growth factor receptor; GEF, guanine nucleotide exchange factor; GRB2, growth factor receptor-bound protein 2; IPSC, inhibitory postsynaptic current; IP_3, inositol 1,4,5-trisphosphate; LPP, lipid phosphate phosphatase; LPA, lysophosphatidic acid; MADD-2, muscle arm development defective-2; PRG, plasticity-related gene; shRNA, short hairpin RNA; SOS, son of sevenless; TRIM, tripartite motif; TRPV5, transient receptor potential cation channel V5.

important in the signal pathway from FGFR1 to Ras (19–21). 80K-H has also been identified as a molecule that interacts with the epithelial Ca^{2+} channel, transient receptor potential cation channel V5 (TRPV5), protein kinase C and MUNC18c (22). Recently, 80K-H has been shown to interact with inositol 1,4,5-trisphosphate (IP_3) receptors and to regulate IP_3-induced calcium release (23). Moreover, it has been reported that 80K-H is one of the genes responsible for autosomal dominant polycystic liver disease (24, 25).

Lysophosphatidic acid (LPA) is a hydrophilic lipid that acts as a ligand for intracellular signaling and induces cell proliferation, retraction, cell survival, migration, and differentiation (26–28). Plasticity-related genes (PRGs), which are specifically expressed in the brain, are transmembrane proteins with lipid phosphate phosphatase (LPP) activity and function as receptors of LPA, resulting in regulation of least five small G-proteins (27, 28). PRG-1 is an important molecule in the control of hippocampal excitability dependent on presynaptic LPA_2 receptor signaling (29). PRG-1 is likely to be a calmodulin (CaM)-interacting protein and is involved in postsynaptic functions regulated by intracellular Ca^{2+} signaling (30). Deletion of *Prg-1* in mice leads to epileptic seizures and augmentation of excitatory postsynaptic current (EPSC) but not inhibitory postsynaptic current (IPSC) (29). *In utero* electroporation of PRG-1 into deficient animals revealed that PRG-1 modulates excitation at the synaptic junction (29).

Based on database analysis of TRIM family proteins, we found that TRIM67, which is selectively expressed in the cerebellum, is a novel member of the TRIM protein family. The amino acid sequence of TRIM67 is similar to that of TRIM9, which has already been reported to be highly expressed in the brain. In this study, with the aim of elucidating the molecular function of TRIM67, we performed yeast two-hybrid screening using TRIM67 as bait and identified PRGs and 80K-H as TRIM67-interacting proteins. We found that TRIM67 regulates PRG-1 and 80K-H, which is involved in the activation of Ras, suggesting that TRIM67 negatively regulates Ras in cell proliferation and differentiation of neural precursor cells.

EXPERIMENTAL PROCEDURES

Cloning and Plasmid Construction—Mouse TRIM67, TRIM9, 80K-H, PRG-1, and PRG-2 cDNA were amplified by polymerase chain reaction (PCR) from a mouse brain cDNA library using PCR primers: 5′-GCGATGGAGGAGGAGCTGAAGTGC-3 (TRIM67 forward), 5′-AGGCTAGTTGCCTGACAGCTTTGG-3 (TRIM67 reverse), 5′-CCCATGGAAGAGATGGAAGAAGAG-3 (TRIM9 forward), 5′-CCCTCACGGAGCTGGGGCTTGGGG-3. (TRIM9 reverse), 5′-GGGATGCTGCTGCTGCTACTACTAC-3 (80K-H forward), 5′-AGGCTACAGCTCGTCATGGTCCCCATCAC-3 (80K-H reverse), 5′-TGCATGCAACGCGCTGGT-3 (PRG-1 forward), 5′-ATCCTTATAAGCCCGCGTGGG-3 (PRG-1 reverse), 5′-ACCATGCTTGCTATGAAGGAG-3 (PRG-2 forward), and 5′-GGCTTAGTCCTGGTACCTCCT-3 (PRG-2 reverse). The amplified fragments were subcloned into pBluescript II SK^+ (Stratagene, La Jolla, CA), and the sequences were verified. The resulting cDNA fragments were subcloned into pCGN-HA, p3×FLAG, pBTM116 and pMX-puro. TRIM67 and TRIM9 cDNAs lacking the RING domain (TRIM67(ΔR) and TRIM9(ΔR)) were amplified by PCR and subcloned into pCGN-HA.

Yeast Two-hybrid Screening—Complementary DNA encoding the full length of TRIM67 or TRIM9(ΔR) was fused in-frame to the nucleotide sequence for the LexA domain (Clontech Laboratories, Inc. Mountain View, CA) in the yeast two-hybrid vector pBTM116. To screen for proteins that interact with TRIM67, we transfected yeast strain L40 (Invitrogen, Carlsbad, CA) stably expressing the corresponding pBTM116 vector with a mouse brain cDNA library in pACT (Clontech) by the lithium acetate method.

Cell Culture—HEK293T, HeLa, and N1E-115 cells (ATCC, Manassas, VA) were maintained in Dulbecco's modified Eagle's medium (Sigma-Aldrich) supplemented with penicillin (100 units/ml), streptomycin (100 μg/ml) and 10% heat-inactivated fetal calf serum (Invitrogen, Paisley, UK) at 37 °C in a humidified incubator with 5% CO_2 atmosphere.

Immunoblot Analysis and Immunoprecipitation—HEK293T cells were transfected by the calcium phosphate method and then cultured for 48 h. The cells were lysed in a solution containing 50 mM Tris-HCl (pH 7.4), 150 mM NaCl, 1% Nonidet P-40, leupeptin (10 μg/ml), 1 mM phenylmethylsulfonyl fluoride, 400 μM Na_3VO_4, 400 μM EDTA, 10 mM NaF, and 10 mM sodium pyrophosphate. The cell lysates were immunoprecipitated with antibodies and protein A-Sepharose (GE Healthcare Bioscience Corp., Piscataway, NJ). Immunoblot analysis was performed with the following primary antibodies: anti-FLAG (1 μg/ml; M2 or M5, Sigma), anti-HA (1 μg/ml; HA.11/16B12, Covance, Princeton, NJ), rabbit anti-TRIM67 (1:100 dilution, Abcam, Cambridge, MA), rabbit anti-80K-H (1:600 dilution; H-195, Santa Cruz Biotechnology, Santa Cruz, CA), rabbit anti-PRG-1 (1 μg/ml; Millipore, Billerica, MA), anti-β-actin (0.2 μg/ml; AC15, Sigma).

Protein Stability Assay with Cycloheximide—Cells were cultured with cycloheximide (Sigma) at the concentration of 50 μg/ml and then incubated for various times. Cell lysates were then subjected to SDS-PAGE and immunoblot analysis with antibodies to 80K-H, PRG-1, FLAG, and β-actin.

Generation of Recombinant Protein and Antibody—Glutathione *S*-transferase (GST)-fusion proteins including 37–101, 121–155, 171–221, and 245–301 amino acid residues of mouse TRIM67 were expressed in XL-10 cells using pGEX4T-2 plasmid vector (GE Healthcare) and then purified by reduced glutathione-Sepharose beads (GE Healthcare). The recombinant proteins were used as immunogen in rabbits. A rabbit polyclonal anti-TRIM67 antibody was affinity-purified using a recombinant TRIM67-conjugated Sepharose 4B column. GST-tagged TRIM67, 80K-H, and PRG-1 were expressed in XL-10 Blue cells and then purified by reduced glutathione-Sepharose beads. His_6-FLAG-tagged 80K-H was expressed in *Escherichia coli* strain BL21 (DE3) (Invitrogen) and then purified by using ProBond metal affinity beads (Invitrogen).

Ni-NTA Pull-down Assay—Cell lysates containing 8 M urea were used for purification of His_6-ubiquitin-conjugated proteins by chromatography on ProBond resin (Invitrogen), and proteins were then eluted from the resin with a solution con-

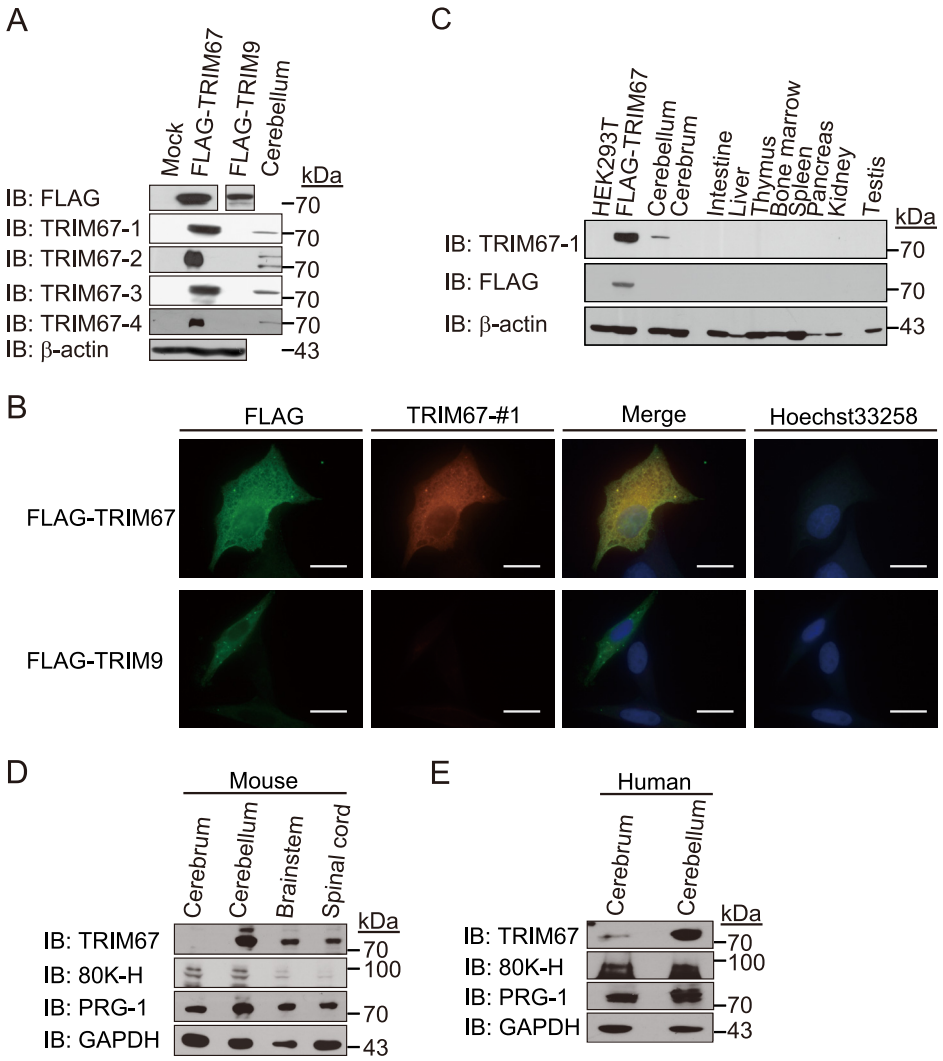

FIGURE 1. **Localization of TRIM67 in the cerebellum and HeLa cells.** *A*, generation of anti-TRIM67 polyclonal antibodies. Four lots of anti-TRIM67 antibodies (anti-TRIM67–1 to -4) were established. The lysates from cells transfected with an expression vector encoding FLAG-tagged TRIM67 or FLAG-tagged TRIM9 or the lysate from the cerebellum were used for immunoblot analysis with these antibodies. β-actin is shown as a loading control. *B*, immunofluorescence analysis of TRIM67. The cells were fixed and stained with antibodies to FLAG (*green*), TRIM67 (*red*), and Hoechst33258 (*blue*). Anti-FLAG staining (*green*) showed the subcellular localization of FLAG-TRIM67 or TRIM9 expressed in HeLa cells. Staining using anti-TRIM67–1 antibody (*red*) showed the cytoplasmic expression of TRIM67. Scale bar, 10 μm. *C*, tissue expression of TRIM67 in mice. The lysates from several tissues were subjected to immunoblot analysis with anti-TRIM67 antibody. β-Actin is shown as a loading control. *D*, expression of TRIM67 in mouse brain tissues. Lysates from cerebrum, cerebellum, brain stem, and spine tissues were subjected to immunoblot analysis with anti-TRIM67–1, -80K-H, and -PRG-1 antibodies. GAPDH is shown as a loading control. *E*, expression of TRIM67 in the human brain. Lysates from the cerebrum and cerebellum were subjected to immunoblot analysis with anti-human TRIM67, -80K-H, and PRG-1 antibodies. GAPDH is shown as a loading control.

taining 50 mM sodium phosphate buffer (pH 8.0), 100 mM KCl, 20% glycerol, 0.2% Nonidet P-40, and 200 mM imidazole.

In Vitro Pull-down Assay—GST-TRIM67 (10 μg), anti-TRIM67 antibody (10 μg) and protein A-Sepharose beads (10 μl) were mixed in binding buffer containing 50 mM Tris-HCl (pH 7.4), 150 mM NaCl, and 0.1% Triton X for 30 min at 4 °C. The beads were then incubated with GST-80K-H (2 μg) in binding buffer for 30 min at 4 °C. The resin was washed five times with the buffer and then boiled in SDS sample buffer. Immunoblot analysis was performed with anti-80K-H antibody.

N1E-115 cells were lysed in a solution containing 50 mM Tris-HCl (pH 7.4), 150 mM NaCl, 1% Nonidet P-40, leupeptin (10 μg/ml), 1 mM phenylmethylsulfonyl fluoride, 400 μM Na_3VO_4, 400 μM EDTA, 10 mM NaF, and 10 mM sodium pyrophosphate. The cell lysates were immunoprecipitated with anti-80K-H or anti-PRG-1 antibody and protein A-Sepharose. The resin was washed five times with the buffer and was then mixed with GST-TRIM67 (5 μg) in a buffer containing 50 mM Tris-HCl (pH 7.4), 150 mM NaCl, and 0.1% Triton X for 30 min at 4 °C. The resin was washed five times with the buffer and then boiled in SDS sample buffer. Immunoblot analysis was performed with anti-TRIM67 antibody.

Establishment of Stable Transfectants by Using a Retrovirus Expression System—Complementary DNAs were subcloned into pMX-puro (kindly provided by T. Kitamura, University of Tokyo) (31). The resulting vectors were used to transfect Plat-E cells, and then recombinant retroviruses were generated (32). Forty-eight hours after transfection, culture supernatants were harvested and then used for infection into N1E-115 and HeLa cells in which mCAT-1 is stably expressed (33). The infection was carried out in the presence of polybrene at 8 μg/ml (Sigma).

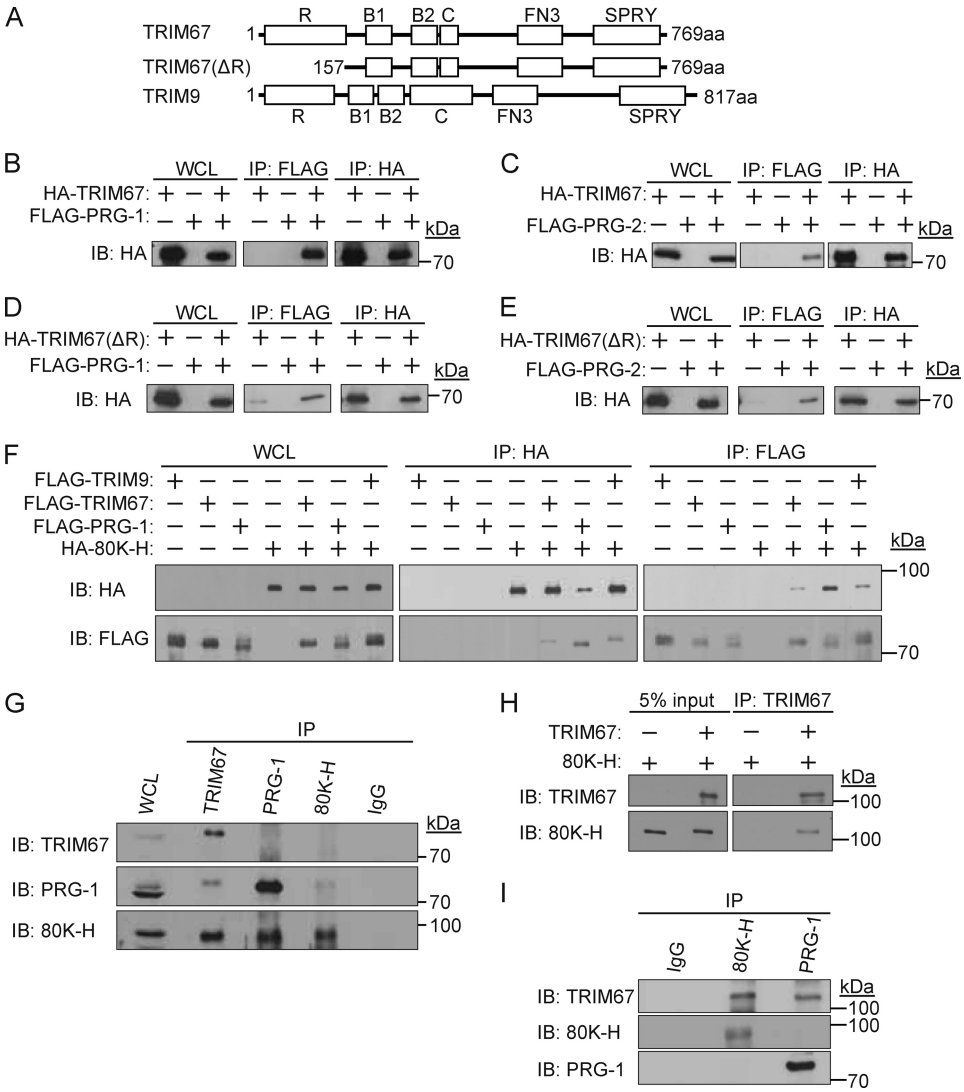

FIGURE 2. **Interaction between TRIM67 and PRG-1, PRG-2, or 80K-H.** *A*, schematic structures of TRIM67 and TRIM9. *R*, RING-finger domain; *B1*, B-box domain 1; *B2*, B-box domain 2; *C*, coiled-coil domain; *FN3*, fibronection type III repeat; *SPRY*, SPRY domain. *B*, interaction between TRIM67 and PRG-1. HA-tagged TRIM67 was expressed in HEK293T cells with or without FLAG-tagged PRG-1, followed by immunoprecipitation (*IP*) with anti-FLAG antibody. Immunoprecipitates were subjected to immunoblot (*IB*) analysis with anti-HA or FLAG antibody. *C*, interaction between TRIM67 and PRG-2. HA-tagged TRIM67 was expressed in HEK293T cells with or without FLAG-tagged PRG-2, followed by immunoprecipitation with anti-FLAG antibody. Immunoprecipitates were subjected to immunoblot analysis with anti-HA or FLAG antibody. *D*, interaction between TRIM67 lacking the RING domain (TRIM67(ΔR)) and PRG-1. HA-tagged TRIM67(ΔR) was expressed in HEK293T cells with or without FLAG-tagged PRG-1, followed by immunoprecipitation with anti-FLAG antibody. Immunoprecipitates were subjected to immunoblot analysis with anti-HA or FLAG antibody. *E*, interaction between TRIM67(ΔR) and PRG-2. HA-tagged TRIM67(ΔR) was expressed in HEK293T cells with or without FLAG-tagged PRG-1, followed by immunoprecipitation with anti-FLAG antibody. Immunoprecipitates were subjected to immunoblot analysis with anti-HA or FLAG antibody. *F*, TRIM67, TRIM9, and PRG-1 bind to 80K-H. FLAG-tagged TRIM67, FLAG-tagged TRIM9, or FLAG-tagged PRG-1 was expressed in HEK293T cells with or without HA-tagged 80K-H, followed by immunoprecipitation with anti-FLAG antibody. Immunoprecipitates were subjected to immunoblot analysis with anti-HA or FLAG antibody. *G*, interaction of endogenous TRIM67 with PRG-1 and 80K-H in N1E-115 cells. Cell lysates were immunoprecipitated with anti-TRIM67, anti-PRG-1, or anti-80K-H antibody and then immunoblotted with anti-TRIM67, anti-PRG-1, or anti-80K-H antibody. *H*, *in vitro* binding assay using purified recombinant TRIM67 and 80K-H proteins. Each protein was mixed in the binding buffer and rotated for 1 h. The mixture was immunoprecipitated with anti-TRIM67 and then immunoblotted with anti-TRIM67 or anti-80K-H antibody. *I*, interaction between recombinant TRIM67 and purified 80K-H and PRG-1 from the N1E-115 cell line. Endogenous 80K-H and PRG-1 were immunoprecipitated from N1E-115 cells using anti-80K-H or anti-PRG-1 antibody, mixed with recombinant TRIM67 and then rotated for 1 h. Immunoprecipitates were subjected to immunoblot analysis with anti-TRIM67, anti-80K-H or anti-PRG-1 antibody.

The infected clones were expanded and selected in a medium containing puromycin (5 μg/ml).

Ras Activation Assay—The amount of Ras activation was determined according to the protocol of manufacturer (Thermo Fisher Scientific, Bonn, Germany).

RNA Interference—pSUPER-retro-puro vector was purchased from OligoEngine (Seattle, WA). A short hairpin RNA (shRNA) for mouse TRIM67 or 80K-H mRNA was designed according to a previous report (34) and chemically synthesized (Invitrogen). pSUPER-retro-puro containing an shRNA for mouse TRIM67 or 80K-H sequences was constructed according to the manufacturer's protocol: shTRIM67–1, 5′-GAAGCTACGCCAGTCCACG-3′; shTRIM67–2, 5′-CAGATCTCAGACGCCTTG-3′; sh80K-H-1, 5′-GTGGTGACCAGCACCACGG-3′; sh80K-H-2, 5′-GCCATGTTCCTGAGGCCCC-3′. We also used a scrambled shRNA as a negative control with no significant homology to any known gene sequences in human and mouse genomes. All shRNA sequences were controlled for

their specificity by using the BLAST database. All of the above sequences were inserted into the BglII and HindIII enzyme sites of pSUPER-retro-puro vector. Approximately 50% confluent HEK293 cells in 100-mm dishes were transfected with 10 μg of pSUPER-retro-puro-TRIM67, pSUPER-retro-puro-80K-H, or scrambled shRNA vector together with 10 μg of amphotrophic packaging plasmid pCL10A1 using the calcium phosphate method. Forty-eight hours after transfection, culture supernatant containing retrovirus was collected, and retroviral supernatant was added to N1E-115 cells in 60-mm dishes with polybrene (8 μg/ml, Sigma). Cells were cultured with puromycin (5 μg/ml) for 1 week. After selection in a medium containing puromycin, the resulting cell lines were checked by immunoblot analysis with anti-TRIM67 and anti-80K-H antibodies.

Immunofluorescence Staining—HeLa cells grown on a glass cover were fixed for 10 min at room temperature with 2% formaldehyde in PBS and then incubated for 1 h at room temperature with a primary antibody in PBS containing 0.1% bovine serum albumin and 0.1% saponin. The cells were then incubated with Alexa488-labeled goat polyclonal antibody to mouse IgG or Alexa546-labeled goat polyclonal antibody to rabbit IgG (Invitrogen) at a dilution of 1:1,000. The cells were further incubated with Hoechst33258 (0.3 μg/ml) in PBS for 30 s followed by extensive washing with PBS and then photographed with a CCD camera (DP71, Olympus, Japan) attached to an Olympus BX51 microscope.

Human Tissue Samples—Tissues from patients who gave informed consent under the guidelines of the Hokkaido University Hospital Ethics Committee were used for this study. All excised tissues were immediately placed in liquid nitrogen and stored at −80 °C until further analysis.

Statistical Analysis—Student's *t* test was used to determine the statistical significance of experimental data.

RESULTS

Tissue Distribution and Subcellular Localization of TRIM67—Since we found that TRIM67 seems to be selectively expressed in the brain, based on database analysis (BioGPS), we isolated mouse full-length TRIM67 cDNA. By using this cDNA, recombinant TRIM67 protein was generated to use it as an immunogen. We generated several anti-TRIM67 antibodies (TRIM67–1–4) by immunization of recombinant TRIM67 into rabbits (Fig. 1*A*). The amino acid sequence of TRIM67 is similar to that of TRIM9: the percent identity between TRIM67 and TRIM9 is 64.8%. Immunoblot analysis showed that four established anti-TRIM67 antibodies recognize FLAG-tagged TRIM67 but not FLAG-tagged TRIM9, indicating that these anti-TRIM67 antibodies are specific to TRIM67. In addition, immunofluorescence analysis using FLAG-tagged TRIM67- or TRIM9-transfected HeLa cells showed that the staining pattern with anti-TRIM67 antibody is similar to that with anti-FLAG antibody, by which FLAG-tagged TRIM67 is stained in the cytosol or the vesicles, and that anti-TRIM67 antibody does not recognize FLAG-tagged TRIM9, which is stained in the cytosol and in the dots by anti-FLAG antibody (Fig. 1*B*). Immunoblot analysis using several mouse and human tissues showed that TRIM67 is highly expressed in the cerebellum (Fig. 1, *C* and *E*). Moreover, immunoblot analysis showed that TRIM67 is also highly expressed in the brainstem and spinal cord, whereas TRIM67 is weakly expressed in the cerebrum (Fig. 1, *C* and *D*).

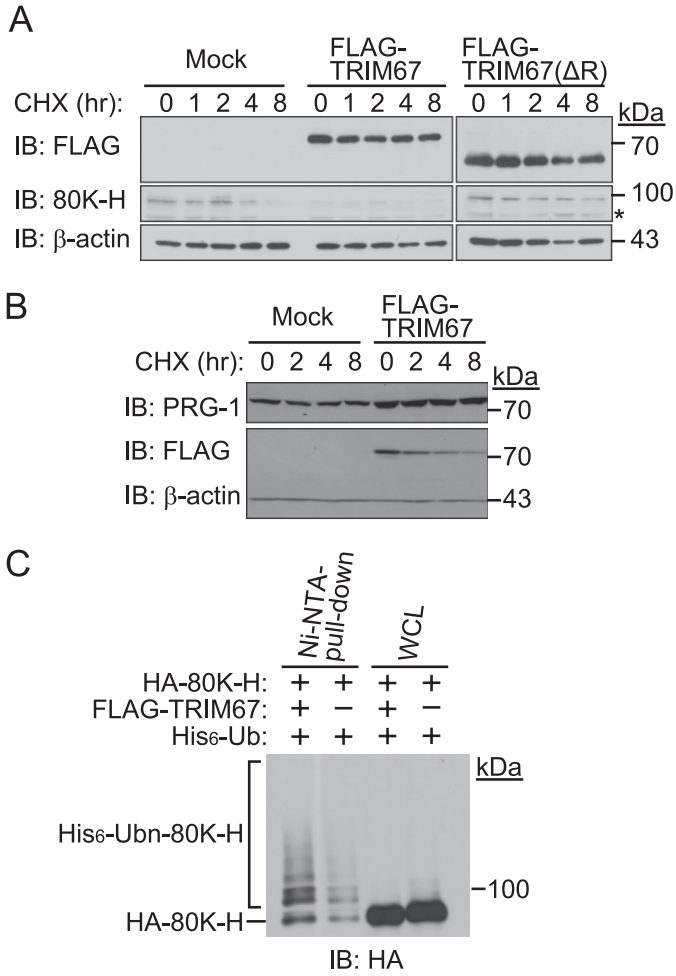

FIGURE 3. **TRIM67 promotes ubiquitination and degradation of 80K-H but not those of PRG-1.** *A*, protein stability assay of 80K-H by overexpression of TRIM67. N1E-115 cells stably expressing FLAG-tagged TRIM67 or FLAG-tagged TRIM67(ΔR) were incubated with cycloheximide (CHX) (50 μg/ml) for 0, 1, 2, 4, or 8 h. The cell lysates were subjected to immunoblot (*IB*) analysis with anti-FLAG, anti-80K-H or anti-β-actin antibody. β-Actin is shown as a loading control. An *asterisk* indicates a nonspecific signal. *B*, protein stability assay of PRG-1 by overexpression of TRIM67. N1E-115 cells stably expressing FLAG-tagged TRIM67 were incubated with CHX (50 μg/ml) for 0, 2, 4, or 8 h. The cell lysates were subjected to immunoblot analysis with anti-FLAG, anti-PRG-1, or anti-β-actin antibody. β-Actin is shown as a loading control. *C*, *in vivo* ubiquitination assay of 80K-H by TRIM67. HEK293T cells were transfected with plasmids encoding FLAG-TRIM67, HA-80K-H and His_6-tagged ubiquitin. Two days after transfection, the cells were cultured with the proteasome inhibitor MG132 (2 μM) for 15 h. The cell lysates were subjected to Ni-NTA pull-down to purify the proteins modified by His_6-ubiquitin (His_6-Ub), followed by immunoblot analysis with anti-HA.

Identification of TRIM67-binding Proteins—To identify proteins that interact with TRIM67 and TRIM9, we screened a mouse brain cDNA library with TRIM67 as a bait by the yeast two-hybrid system. We identified PRG-2 as a TRIM67-interacting protein (supplemental Fig. S1*A*). We further screened the mouse brain cDNA library with TRIM9(ΔR), which lacks the RING domain necessary for ubiquitin ligase activity, as a bait and isolated PRG-1 and 80K-H (Fig. 2*A*, supplemental Fig. S1, *B* and *C*). Because it has been reported that PRGs have five members, PRG-1 as another PRG member also was evaluated to examine the interaction with TRIM67. We transfected expres-

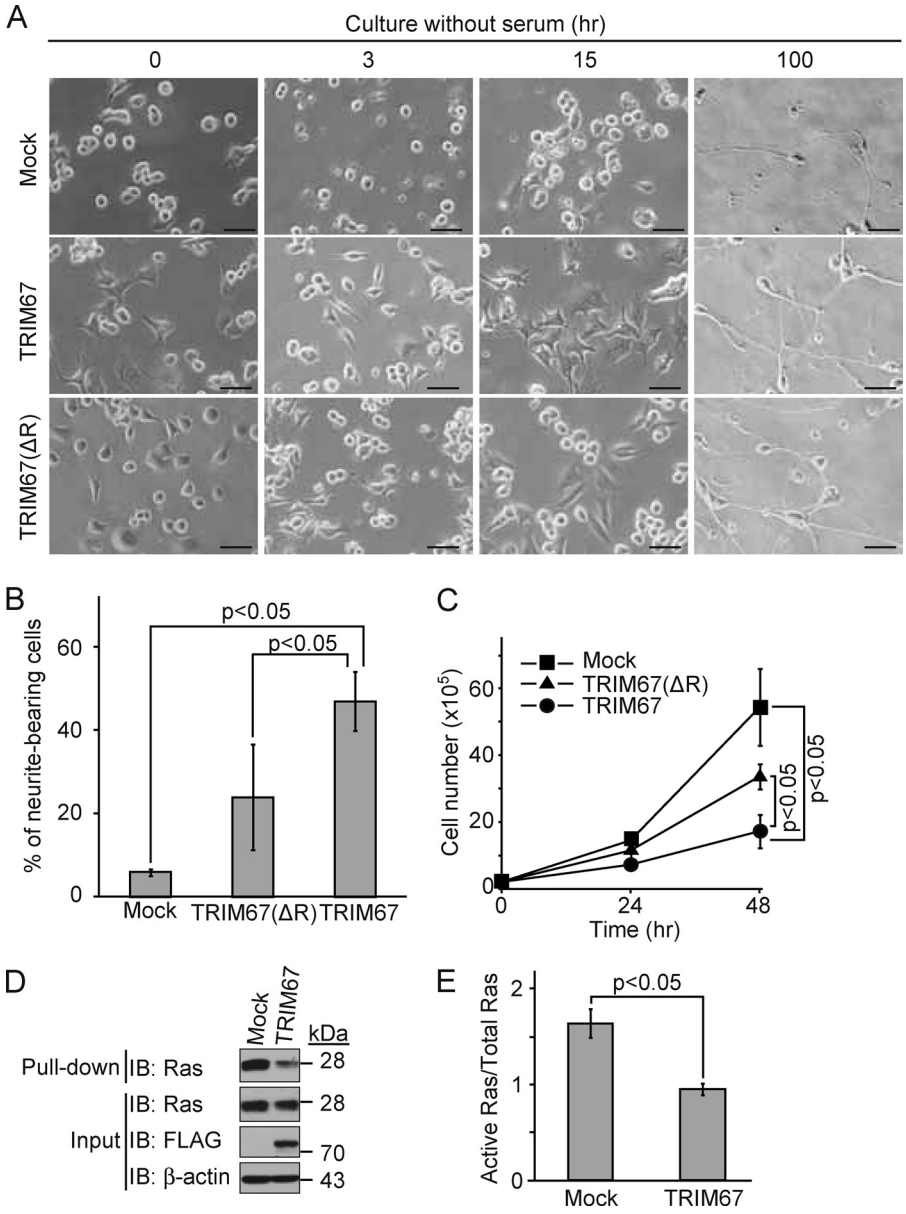

FIGURE 4. **Effect of TRIM67 overexpression in N1E-115 cells.** *A,* Culture of N1E-115 cells stably expressing FLAG-tagged TRIM67 in the absence of serum. N1E-115 cells stably expressing FLAG-tagged TRIM67 or FLAG-tagged TRIM67(ΔR) were observed at 3, 15, and 100 h after removing serum. *Scale bar*, 100 μm. *B*, percentage of neurite-bearing cells in the presence of serum. Cells that have neurites longer than the diameter of their cell body were counted and the percentages of cell number with neurites to that without neurites were calculated. The percentage of cells with neurites is shown as mean ± S.D. of values from three independent experiments. *p* values for the indicated comparisons were determined by Student's *t* test. *C*, overexpression of TRIM67 causes delay of cell growth. Cell lines were seeded at 1×10^5 cells and harvested for determination of cell number at the indicated times. Data are means ± S.D. of values from three independent experiments. *D*, effect of TRIM67 on Ras activation. N1E-115 cells stably expressing FLAG-TRIM67 were precipitated with beads bound to the Ras-binding domain of Raf and then subjected to immunoblot analysis with anti-FLAG, anti-Ras, and anti-β-actin antibodies. β-Actin is shown as a loading control. *E*, quantification of Ras activation assay. The ratio of active Ras that interacts with the Ras-binding domain of Raf to total Ras was calculated. Data are means ± S.D. of values from three independent experiments obtained in *D*.

sion vectors encoding HA-tagged TRIM67 and FLAG-tagged PRG-1 or FLAG-tagged PRG-2 into HEK293T cells, followed by immunoprecipitation and immunoblotting with anti-FLAG or HA antibody (Fig. 2, *B* and *C*). Immunoblot analysis showed that HA-tagged TRIM67 specifically interacts with FLAG-tagged PRG-1 and FLAG-tagged PRG-2. Moreover, HA-tagged TRIM67(ΔR) specifically interacted with FLAG-tagged PRG-1 and FLAG-tagged PRG-2, suggesting that the RING domain is not required for interaction between TRIM67 and PRG-1/2 (Fig. 2*D* and *E*). We also checked the interactions among 80K-H, PRG-1, TRIM67, and TRIM9. FLAG-tagged TRIM67, FLAG-tagged TRIM9 FLAG-tagged PRG-1 and/or HA-tagged 80K-H were transfected into HEK293T cells, and cell lysates were subjected to immunoprecipitation and immunoblotting with antibodies to FLAG or HA. Immunoblot analysis showed that 80K-H interacts with TRIM67, TRIM9, and PRG-1 (Fig. 2*F*). Furthermore, we verified interaction among endogenous TRIM67, PRG-1, and 80K-H by using the mouse neuroblastoma cell line N1E-115, in which endogenous TRIM67 is likely to be expressed (Fig. 2*G*). Immunoprecipitation analysis showed that anti-TRIM67 immunoprecipitates contained endogenous PRG-1 and 80K-H. Anti-PRG-1 and anti-80K-H

immunoprecipitates contained enodogenous 80K-H and PRG-1, respectively. However, anti-PRG-1 and anti-80K-H immunoprecipitates did not contain endogenous TRIM67, suggesting that anti-PRG-1 and anti-80K-H antibodies recognize the binding regions between PRG-1 and TRIM67 and between 80K-H and TRIM67. Furthermore, *in vitro* binding assays showed direct interactions between TRIM67 and 80K-H using each purified recombinant protein (Fig. 2*H*). However, we could not show a direct interaction between TRIM67 and PRG-1 by an *in vitro* pull-down assay (data not show). We performed a pull-down assay using recombinant TRIM67 and purified 80K-H and PRG-1 prepared from N1E-115 cells (Fig. 2*I*). Immunoblot analysis showed that recombinant TRIM67 interacts with 80K-H and PRG-1 purified from N1E-115 cells. These findings indicate that TRIM67 directly interacts with 80K-H and suggest that TRIM67 interacts with PRG-1 via an unknown modification or unknown adaptor molecule.

TRIM67 Promotes Ubiquitination and Degradation of 80K-H but Not Those of PRG-1—We first established N1E-115 cell lines stably expressing FLAG-tagged TRIM67 and FLAG-tagged TRIM67(ΔR) (Fig. 3*A*). A protein stability assay with cycloheximide using these cell lines was performed to examine the effect of stability of 80K-H by TRIM67. Ectopic expression of TRIM67 resulted in rapid degradation of endogenous 80K-H compared with mock, whereas TRIM67(ΔR) delayed the degradation of 80K-H, suggesting that the RING domain of TRIM67 is required for acceleration of degradation of 80K-H (Fig. 3*A*). Interestingly, the stability of PRG-1 was increased by TRIM67, suggesting that TRIM67 stabilizes PRG-1 possibly via their interaction (Fig. 3*B*). Since TRIM67 promoted degradation of 80K-H, we performed an *in vivo* ubiquitination assay of 80K-H in the presence of TRIM67. The *in vivo* ubiquitination assay showed that TRIM67 overexpression enhances ubiquitination of 80K-H, suggesting that TRIM67 promotes ubiquitination of 80K-H and then contributes to the proteasomal degradation of 80K-H (Fig. 3*C*).

Neural Differentiation of N1E-115 by TRIM67—Because it has been reported that serum starvation results in neurite outgrowth and differentiation of N1E-115 cells (35) and that PRG-1 mediates neurite outgrowth (27, 36), we analyzed the physiological roles of TRIM67 using N1E-115 cells. To clarify the functional effect of TRIM67 on differentiation of N1E-115 cells, we investigated morphological change of N1E-115 cells under a serum starvation condition (Fig. 4*A*). In the presence of serum, TRIM67 overexpression induced a flattened shape and extended neurites compared with the mock cell line (Fig. 4, *A* and *B*). After serum starvation for 24 h, TRIM67 or TRIM67(ΔR) overexpression increased the number of neurite-bearing cells, but the effect of TRIM67(ΔR) was weaker than that of TRIM67, suggesting that the RING domain is partially required for neuritogenesis (Fig. 4, *A* and *B*). Furthermore, TRIM67 or TRIM67(ΔR) overexpression attenuated cell proliferation, followed by neural differentiation (Fig. 4*C*).

Because it has been reported that 80K-H and PRG-1 regulate Ras activity (28, 37), we examined the biological function of TRIM67 in a Ras activation. We pulled-down activated Ras with the Ras-binding domain of Raf using stable N1E-115 cell line overexpressing FLAG-TRIM67 and investigated the amount of the GTP-bound active form Ras. The Ras activation assays showed that Ras is inactivated in N1E-115 cells by overexpression of TRIM67, suggesting that TRIM67 causes delayed cell proliferation and enhanced neuritogenesis because of inactivation of Ras via inhibition of 80K-H (Fig. 4, *D* and *E*).

Up-regulation of Ras Activity by Knockdown of TRIM67—To examine the physiological role of TRIM67, we knocked down endogenous TRIM67 in N1E-115 cells by using two independent targeting sequences (Fig. 5*A*). Knockdown of TRIM67 caused up-regulation of 80K-H, indicating that TRIM67 may be an E3 ubiquitin ligase for 80K-H (Fig. 5*A*). Furthermore, knockdown of TRIM67 in N1E-115 cells slightly but significantly reduced the number of neurite-bearing cells in the presence of

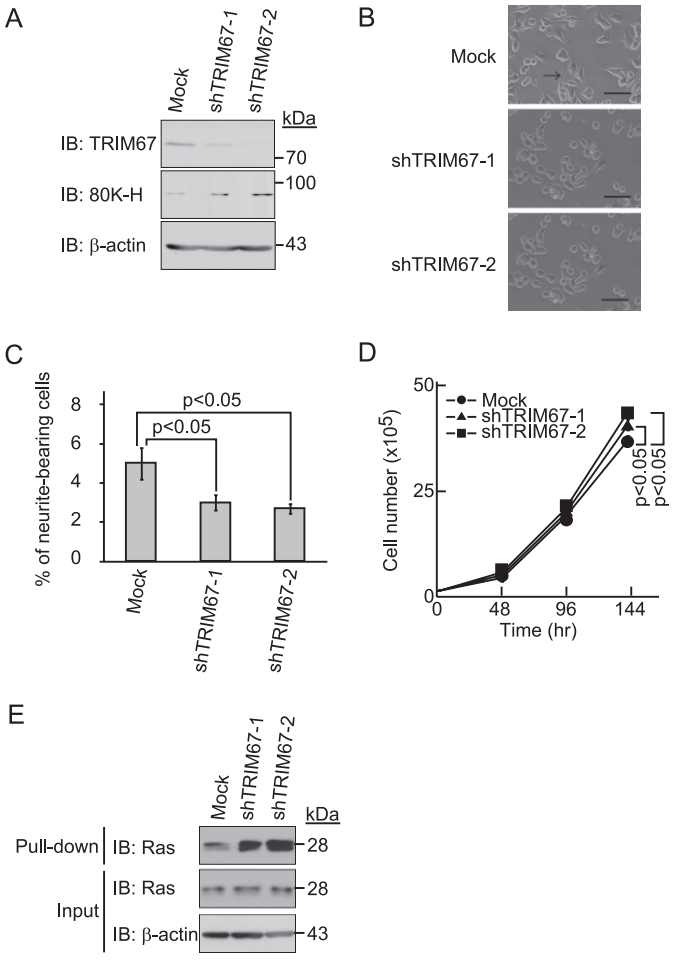

FIGURE 5. **Knockdown of TRIM67 in N1E-115 cells.** *A*, establishment of TRIM67 knocked-down cell lines. Endogenous TRIM67 was knocked down in N1E-115 cell lines (shTRIM67–1 and 2) by using two independent targeting sequences. Cell lysates were immunoblotted with anti-TRIM67, anti-80K-H, or anti-β-actin antibodies. *B*, morphological changes of TRIM67 knocked-down N1E-115 cell lines in the presence of serum for 48 h. *Arrows* show neurite-bearing cells. *Scale bar*, 100 μm. *C*, percentage of neurite-bearing cells in TRIM67 knocked-down N1E-115 cell lines in the presence of serum for 48 h. Data are means ± S.D. of values from three independent experiments. *D*, knockdown of TRIM67 caused acceleration of cell growth. Cell lines were seeded at 1×10^5 cells and harvested for determination of cell number at the indicated times. Data are means ± S.D. of values from three independent experiments. *E*, effect of TRIM67 knockdown on Ras activation. N1E-115 cells in which TRIM67 was knocked down were precipitated with beads bound to the Ras-binding domain of Raf and then subjected to immunoblot analysis with anti-Ras and anti-β-actin antibodies. β-Actin is shown as a loading control.

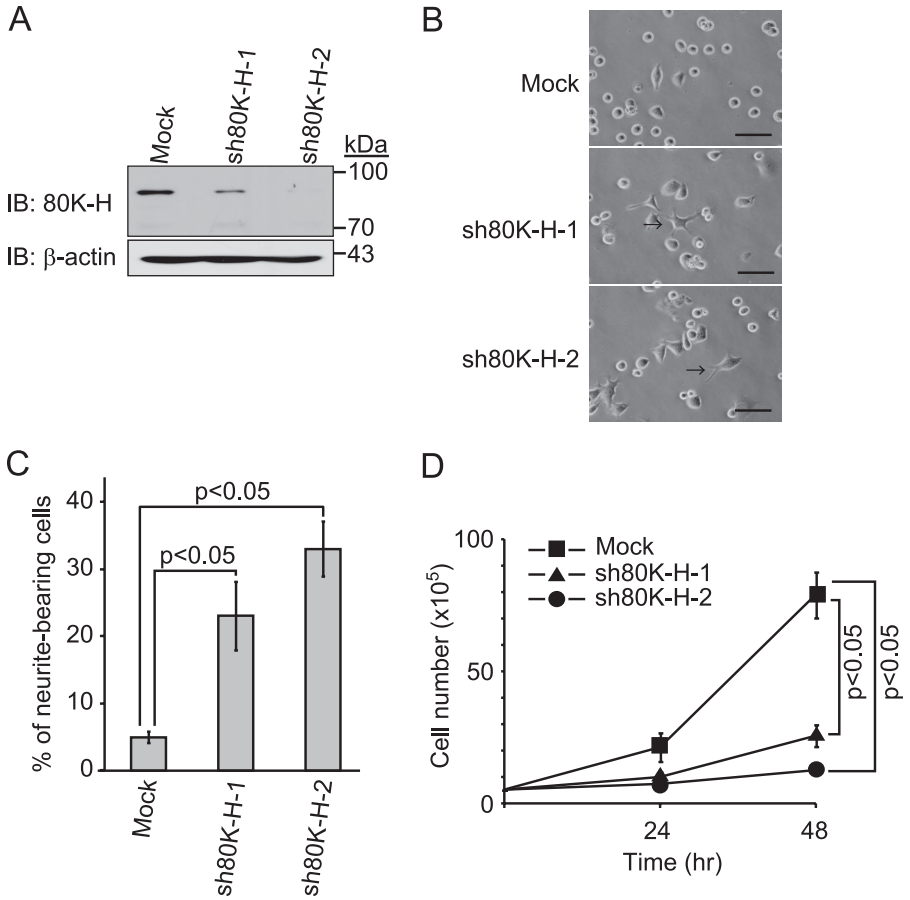

FIGURE 6. **Knockdown of 80K-H in N1E-115 cells.** *A*, establishment of 80K-H knocked-down cell lines. Endogenous 80K-H was knocked down in N1E-115 cell lines (sh80K-H-1 and -2) by using two independent targeting sequences. Cell lysates were immunoblotted with anti-80K-H or anti-β-actin antibodies. *B*, morphological changes of 80K-H knocked-down N1E-115 cell lines in the presence of serum. *Arrows* show neurite-bearing cells. *Scale bar*, 100 μm. *C*, percentage of neurite-bearing cells in 80K-H knocked-down N1E-115 cell lines in the presence of serum. Data are means ± S.D. of values from three independent experiments. *D*, knockdown of 80K-H caused increase in cell growth. Cell lines were seeded at 5×10^5 cells and harvested for determination of cell number at the indicated times. Data are means ± S.D. of values from three independent experiments.

serum (Fig. 5, *B* and *C*). Furthermore, knockdown of TRIM67 caused acceleration of cell growth (Fig. 5*D*). To examine the effect of knockdown of TRIM67 on Ras activation, we compared the amount of active Ras in TRIM67 knocked-down cell lines compared with that in mock cells. Activation of Ras was observed in TRIM67 knocked-down cell lines but not in mock cells (Fig. 5*E*). These findings suggest that TRIM67 negatively regulates Ras activation.

Differentiation of N1E-115 Cells by Knockdown of 80K-H—To clarify the physiological relationship between TRIM67 and 80K-H, we also established two independent 80K-H knocked-down N1E-115 cell lines (Fig. 6*A*). Using these cell lines, we counted the number of neurite-bearing cells in the presence of serum. Knockdown of 80K-H caused an increase in the number of neurite-bearing cells compared with mock cells in the presence of serum (Fig. 6, *B* and *C*). Furthermore, knockdown of 80K-H attenuated cell proliferation (Fig. 6*D*). Given that the physiological phenotype of 80K-H knockdown is similar to that of TRIM67 overexpression and that TRIM67 physically interacts with 80K-H, TRIM67 may function as a negative regulator for 80K-H, resulting in Ras inhibition via degradation of 80K-H followed by growth arrest and neuritogenesis in neural precursor cells.

DISCUSSION

In this study, we identified PRG-1 and 80K-H as TRIM67-interacting proteins. We showed that TRIM67 functioned as a putative E3 ubiquitin ligase for 80K-H and that ectopic expression of TRIM67 induced neurite outgrowth and suppressed growth of N1E-115 cells. Moreover, ectopic expression of TRIM67 down-regulated Ras activity probably via degradation of 80K-H. In contrast, knockdown of TRIM67 attenuated neurite outgrowth in N1E-115 cells and up-regulated Ras activity. The regulation of cell proliferation has been shown to be tightly linked to differentiation in normal cells including neurons and also tumor cells with deregulated proliferation (38, 39). These findings suggest that TRIM67 attenuates cell proliferation and induces morphological changes like neuronal differentiation.

FGF stimulation induces tyrosine phosphorylation of 80K-H, which binds activated FGFR directly and forms a ternary complex with GRB2-SOS, leading to a connection from FGFR to the Ras signal (19, 20, 37). Our studies showed that morphological and biological effects by knockdown of 80K-H were similar to the changes induced by overexpression of TRIM67. These findings indicate that overexpression of TRIM67 in N1E-115 cells may downregulate activation of Ras via degradation of 80K-H.

Furthermore, it has been reported that TRIM9 has an E3 ubiquitin ligase activity and affects the localization of downstream effectors by ubiquitinating Rac guanine nucleotide exchange factor (GEF) (15, 17). Since TRIM67 is structurally similar to TRIM9, TRIM67 may also function as an E3 ubiquitin ligase for 80K-H as a regulator for Ras,. It has been reported that Purkinje cells from IP_3R-deficient mice show abnormal dendritic outgrowth (40). 80K-H interacts with inositol 1,4,5-trisphosphate receptors (IP_3R), regulates IP_3-induced calcium release and consequently contributes to neuronal functions (23). Taken together, the results indicate that IP_3R may be functionally inhibited by TRIM67 through degradation of 80K-H, resulting in regulation of neuronal differentiation.

PRG-1 is highly expressed in the forebrain and in the cerebellar cortex (30). It has been reported that overexpression of PRG-1 induces neurite outgrowth in PC12 cells (36) and that PRG-1 is up-regulated during periods of axonal outgrowth and attenuates LPA-induced axon collapse (27). PRG-1 deficiency results in pathological network synchronization due to a pathological increase of excitatory synaptic transmission (29). In this study, we showed that overexpression of TRIM67 may stabilize endogenous PRG-1, indicating that neurite outgrowth by overexpression of TRIM67 is due to stabilization of PRG-1. Considering that overexpression of TRIM67 in N1E-115 cells causes stabilization of PRG-1, TRIM67 may function as a positive regulator for PRG-1. Because deletion of *prg-1* in mice leads to epileptic seizures, TRIM67 and TRIM9 may be associated with the etiology of epilepsy (29). Hence, it would be interesting to clarify the molecular mechanism of TRIM67 in epilepsy.

The *C. elegans* homolog of TRIM9 or TRIM18 (MID1), which is designated muscle arm development defective-2 (MADD-2), was recently isolated (16, 41). The ventral guidance factor UNC-6/Netrin-1, its receptor unc-40/DCC and MADD-2 induce ventral axon branching in *C. elegans* chemosensory and mechanosensory neurons, indicating that MADD-2 has important roles for axon guidance and branching in the UNC-40-mediated UNC-6/Netrin-1 attraction pathway (16, 17). UNC-6/Netrin-1 inhibits RhoA in embryonic spinal commissural neurons through DCC (42). Taken together, the results indicate that in neuritogenesis and axon guidance, TRIM67 may regulate Ras activity, whereas TRIM9 may regulate Rho activity.

In conclusion, TRIM67 interacts with PRG-1 and 80K-H and affects neurite elongation in neuronal precursor cells. However, it is unclear whether interaction of TRIM67 with PRG-1 and 80K-H contributes to neuronal development. Genetic approaches using transgenic or knock-out mice will be necessary to clarify the relationship between TRIM67 and neuritogenesis. Further functional analysis of TRIM67 at the molecular level would provide therapeutic benefits not only for suppression in axonal injury but also for neurodegenerative diseases.

Acknowledgments—We thank Dr. Toshio Kitamura (Tokyo University) and Dr. Kentaro Hanada (National Institute of Infectious Diseases) for the plasmids and Yuri Soida for help in preparing the manuscript.

REFERENCES

1. Peters, J. M. (1998) SCF and APC: the Yin and Yang of cell cycle-regulated proteolysis. *Curr. Opin. Cell Biol.* **10,** 759–768
2. Hershko, A., and Ciechanover, A. (1998) The ubiquitin system. *Annu. Rev. Biochem.* **67,** 425–479
3. Hershko, A., and Ciechanover, A. (1992) The ubiquitin system for protein degradation. *Annu. Rev. Biochem.* **61,** 761–807
4. Scheffner, M., Nuber, U., and Huibregtse, J. M. (1995) Protein ubiquitination involving an E1-E2-E3 enzyme ubiquitin thioester cascade. *Nature* **373,** 81–83
5. Huibregtse, J. M., Scheffner, M., Beaudenon, S., and Howley, P. M. (1995) A family of proteins structurally and functionally related to the E6-AP ubiquitin-protein ligase. *Proc. Natl. Acad. Sci. U.S.A.* **92,** 2563–2567
6. Freemont, P. S. (2000) RING for destruction? *Curr. Biol.* **10,** R84–87
7. Joazeiro, C. A., and Weissman, A. M. (2000) RING finger proteins: mediators of ubiquitin ligase activity. *Cell* **102,** 549–552
8. Lorick, K. L., Jensen, J. P., Fang, S., Ong, A. M., Hatakeyama, S., and Weissman, A. M. (1999) RING fingers mediate ubiquitin-conjugating enzyme (E2)-dependent ubiquitination. *Proc. Natl. Acad. Sci. U.S.A.* **96,** 11364–11369
9. Aravind, L., and Koonin, E. V. (2000) The U box is a modified RING finger - a common domain in ubiquitination. *Curr. Biol.* **10,** R132–134
10. Cyr, D. M., Höhfeld, J., and Patterson, C. (2002) Protein quality control: U-box-containing E3 ubiquitin ligases join the fold. *Trends Biochem. Sci.* **27,** 368–375
11. Hatakeyama, S., Yada, M., Matsumoto, M., Ishida, N., and Nakayama, K. I. (2001) U box proteins as a new family of ubiquitin-protein ligases. *J. Biol. Chem.* **276,** 33111–33120
12. Meroni, G., and Diez-Roux, G. (2005) TRIM/RBCC, a novel class of 'single protein RING finger' E3 ubiquitin ligases. *Bioessays* **27,** 1147–1157
13. Nisole, S., Stoye, J. P., and Saïb, A. (2005) TRIM family proteins: retroviral restriction and antiviral defence. *Nat. Rev. Microbiol.* **3,** 799–808
14. Rajsbaum, R., Stoye, J. P., and O'Garra, A. (2008) Type I interferon-dependent and -independent expression of tripartite motif proteins in immune cells. *Eur. J. Immunol.* **38,** 619–630
15. Tanji, K., Kamitani, T., Mori, F., Kakita, A., Takahashi, H., and Wakabayashi, K. (2010) TRIM9, a novel brain-specific E3 ubiquitin ligase, is repressed in the brain of Parkinson's disease and dementia with Lewy bodies. *Neurobiol. Dis.* **38,** 210–218
16. Hao, J. C., Adler, C. E., Mebane, L., Gertler, F. B., Bargmann, C. I., and Tessier-Lavigne, M. (2010) The tripartite motif protein MADD-2 functions with the receptor UNC-40 (DCC) in Netrin-mediated axon attraction and branching. *Dev. Cell* **18,** 950–960
17. Song, S., Ge, Q., Wang, J., Chen, H., Tang, S., Bi, J., Li, X., Xie, Q., and Huang, X. (2011) TRIM-9 functions in the UNC-6/UNC-40 pathway to regulate ventral guidance. *J. Genet. Genomics* **38,** 1–11
18. Trombetta, E. S., Simons, J. F., and Helenius, A. (1996) Endoplasmic reticulum glucosidase II is composed of a catalytic subunit, conserved from yeast to mammals, and a tightly bound noncatalytic HDEL-containing subunit. *J. Biol. Chem.* **271,** 27509–27516
19. Klint, P., Kanda, S., and Claesson-Welsh, L. (1995) Shc and a novel 89-kDa component couple to the Grb2-Sos complex in fibroblast growth factor-2-stimulated cells. *J. Biol. Chem.* **270,** 23337–23344
20. Kanai, M., Göke, M., Tsunekawa, S., and Podolsky, D. K. (1997) Signal transduction pathway of human fibroblast growth factor receptor 3. Identification of a novel 66-kDa phosphoprotein. *J. Biol. Chem.* **272,** 6621–6628
21. Mohammadi, M., Dikic, I., Sorokin, A., Burgess, W. H., Jaye, M., and Schlessinger, J. (1996) Identification of six novel autophosphorylation sites on fibroblast growth factor receptor 1 and elucidation of their importance in receptor activation and signal transduction. *Mol. Cell Biol.* **16,** 977–989
22. Hodgkinson, C. P., Mander, A., and Sale, G. J. (2005) Identification of 80K-H as a protein involved in GLUT4 vesicle trafficking. *Biochem. J.* **388,** 785–793
23. Kawaai, K., Hisatsune, C., Kuroda, Y., Mizutani, A., Tashiro, T., and Mikoshiba, K. (2009) 80K-H interacts with inositol 1,4,5-trisphosphate (IP3) receptors and regulates IP3-induced calcium release activity. *J. Biol. Chem.*

284, 372–380
24. Drenth, J. P., te Morsche, R. H., Smink, R., Bonifacino, J. S., and Jansen, J. B. (2003) Germline mutations in PRKCSH are associated with autosomal dominant polycystic liver disease. *Nat. Genet.* **33,** 345–347
25. Li, A., Davila, S., Furu, L., Qian, Q., Tian, X., Kamath, P. S., King, B. F., Torres, V. E., and Somlo, S. (2003) Mutations in PRKCSH cause isolated autosomal dominant polycystic liver disease. *Am. J. Hum. Genet.* **72,** 691–703
26. Mills, G. B., and Moolenaar, W. H. (2003) The emerging role of lysophosphatidic acid in cancer. *Nat. Rev. Cancer* **3,** 582–591
27. Bräuer, A. U., Savaskan, N. E., Kühn, H., Prehn, S., Ninnemann, O., and Nitsch, R. (2003) A new phospholipid phosphatase, PRG-1, is involved in axon growth and regenerative sprouting. *Nat. Neurosci.* **6,** 572–578
28. Bräuer, A. U., and Nitsch, R. (2008) Plasticity-related genes (PRGs/LRPs): a brain-specific class of lysophospholipid-modifying proteins. *Biochim. Biophys. Acta* **1781,** 595–600
29. Trimbuch, T., Beed, P., Vogt, J., Schuchmann, S., Maier, N., Kintscher, M., Breustedt, J., Schuelke, M., Streu, N., Kieselmann, O., Brunk, I., Laube, G., Strauss, U., Battefeld, A., Wende, H., Birchmeier, C., Wiese, S., Sendtner, M., Kawabe, H., Kishimoto-Suga, M., Brose, N., Baumgart, J., Geist, B., Aoki, J., Savaskan, N. E., Bräuer, A. U., Chun, J., Ninnemann, O., Schmitz, D., and Nitsch, R. (2009) Synaptic PRG-1 modulates excitatory transmission via lipid phosphate-mediated signaling. *Cell* **138,** 1222–1235
30. Tokumitsu, H., Hatano, N., Tsuchiya, M., Yurimoto, S., Fujimoto, T., Ohara, N., Kobayashi, R., and Sakagami, H. (2010) Identification and characterization of PRG-1 as a neuronal calmodulin-binding protein. *Biochem. J.* **431,** 81–91
31. Kitamura, T. (1998) New experimental approaches in retrovirus-mediated expression screening. *Int. J. Hematol.* **67,** 351–359
32. Morita, S., Kojima, T., and Kitamura, T. (2000) Plat-E: an efficient and stable system for transient packaging of retroviruses. *Gene Ther.* **7,** 1063–1066
33. Hanada, K., Kumagai, K., Yasuda, S., Miura, Y., Kawano, M., Fukasawa, M., and Nishijima, M. (2003) Molecular machinery for non-vesicular trafficking of ceramide. *Nature* **426,** 803–809
34. Elbashir, S. M., Harborth, J., Weber, K., and Tuschl, T. (2002) Analysis of gene function in somatic mammalian cells using small interfering RNAs. *Methods* **26,** 199–213
35. Kruman, II, Kostenko, M. A., Gordon, R. Ya., Popov, V. I., and Umansky, S. R. (1993) Differentiation and apoptosis of murine neuroblastoma cells N1E115. *Biochem. Biophys. Res. Commun.* **191,** 1309–1318
36. Yamada, M., Shida, Y., Takahashi, K., Tanioka, T., Nakano, Y., and Tobe, T. (2008) Prg1 is regulated by the basic helix-loop-helix transcription factor Math2. *J. Neurochem.* **106,** 2375–2384
37. Goh, K. C., Lim, Y. P., Ong, S. H., Siak, C. B., Cao, X., Tan, Y. H., and Guy, G. R. (1996) Identification of p90, a prominent tyrosine-phosphorylated protein in fibroblast growth factor-stimulated cells, as 80K-H. *J. Biol. Chem.* **271,** 5832–5838
38. Ajioka, I., Martins, R. A., Bayazitov, I. T., Donovan, S., Johnson, D. A., Frase, S., Cicero, S. A., Boyd, K., Zakharenko, S. S., and Dyer, M. A. (2007) Differentiated horizontal interneurons clonally expand to form metastatic retinoblastoma in mice. *Cell* **131,** 378–390
39. Caldon, C. E., Sutherland, R. L., and Musgrove, E. (2010) Cell cycle proteins in epithelial cell differentiation: implications for breast cancer. *Cell Cycle* **9,** 1918–1928
40. Hisatsune, C., Kuroda, Y., Akagi, T., Torashima, T., Hirai, H., Hashikawa, T., Inoue, T., and Mikoshiba, K. (2006) Inositol 1,4,5-trisphosphate receptor type 1 in granule cells, not in Purkinje cells, regulates the dendritic morphology of Purkinje cells through brain-derived neurotrophic factor production. *J. Neurosci.* **26,** 10916–10924
41. Alexander, M., Selman, G., Seetharaman, A., Chan, K. K., D'Souza, S. A., Byrne, A. B., and Roy, P. J. (2010) MADD-2, a homolog of the Opitz syndrome protein MID1, regulates guidance to the midline through UNC-40 in Caenorhabditis elegans. *Dev. Cell* **18,** 961–972
42. Moore, S. W., Correia, J. P., Lai Wing Sun, K., Pool, M., Fournier, A. E., and Kennedy, T. E. (2008) Rho inhibition recruits DCC to the neuronal plasma membrane and enhances axon chemoattraction to netrin 1. *Development* **135,** 2855–2864